Supporting Information

Entropy-Driven Durability Enhancement of PtM_3 (M=Transition Metal) Type Alloy Catalysts for Oxygen Reduction Reaction

*Jiaqi Wang[a], Longhai Zhang[a], Jinhui Liang[a], Yuanhua Tu[a], Huiyu Song[a], Yan Xiang[b], Nianjun Yang[c]，Shijun Liao[a] and Zhiming Cui[a,]**

[a] *Guangdong Provincial Key Laboratory of Fuel Cell Technology, School of Chemistry and Chemical Engineering, South China University of Technology, Guangzhou 510641, Guangdong, China*

[b] *National Key Laboratory of Multi-perch Vehicle Driving Systems, Beijing Key Laboratory of Bio-inspired Energy Materials and Devices, School of Energy and Power Engineering, Beihang University, Beijing 100191, China*

[c]*Department of Chemistry & IMO-IMOMEC，Hasselt University，3590 Diepenbeek，Belgium*

[*]Email: zmcui@scut.edu.cn

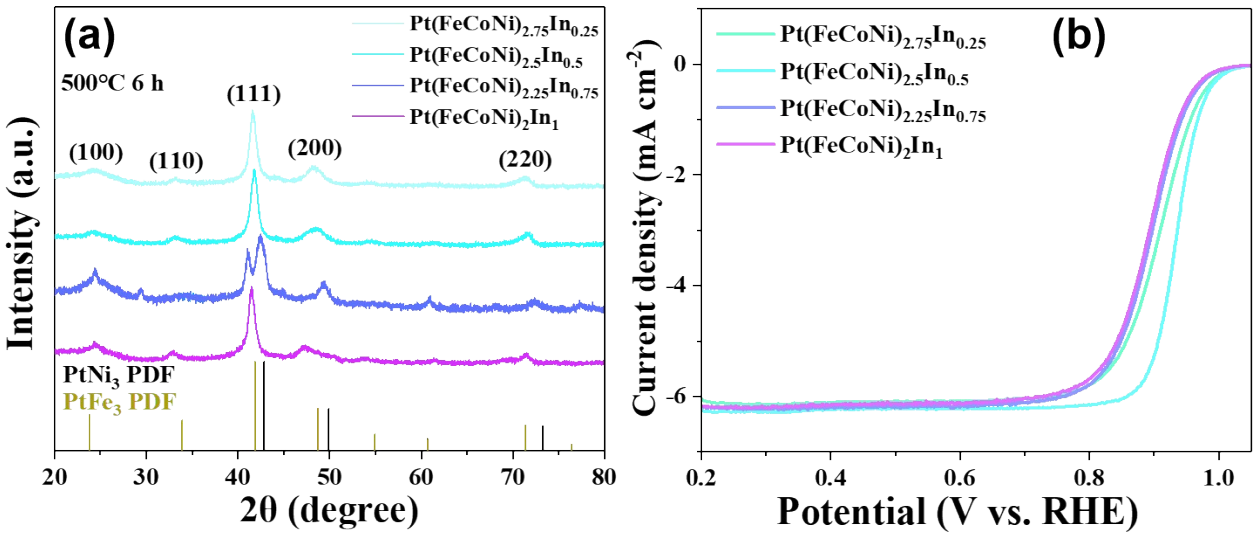

Figure S1. (a) XRD patterns of $Pt(FeCoNi)_{3-x}In_x$ (x=0.25, 0.5, 0.75, 1) annealed at 500°C for 6 h. (b) LSV curves of as-prepared $Pt(FeCoNi)_{3-x}In_x$ (x=0.25, 0.5, 0.75, 1) tested in O_2-saturated 0.1 mol L^{-1} $HClO_4$ at a rotation speed of 1,600 rpm.

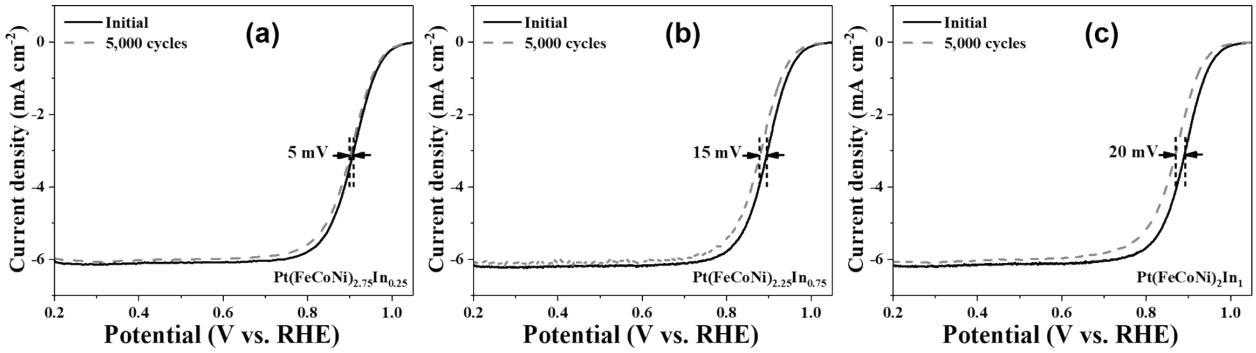

Figure S2. LSV curves of $Pt(FeCoNi)_{3-x}In_x$ (x=0.25, 0.75, 1) at the beginning and after 5,000 ADT cycles, tested in O_2-saturated 0.1 mol L^{-1} $HClO_4$ at a rotation speed of 1,600 rpm: (a) x=0.25; (b) x=0.75; (c) x=1;

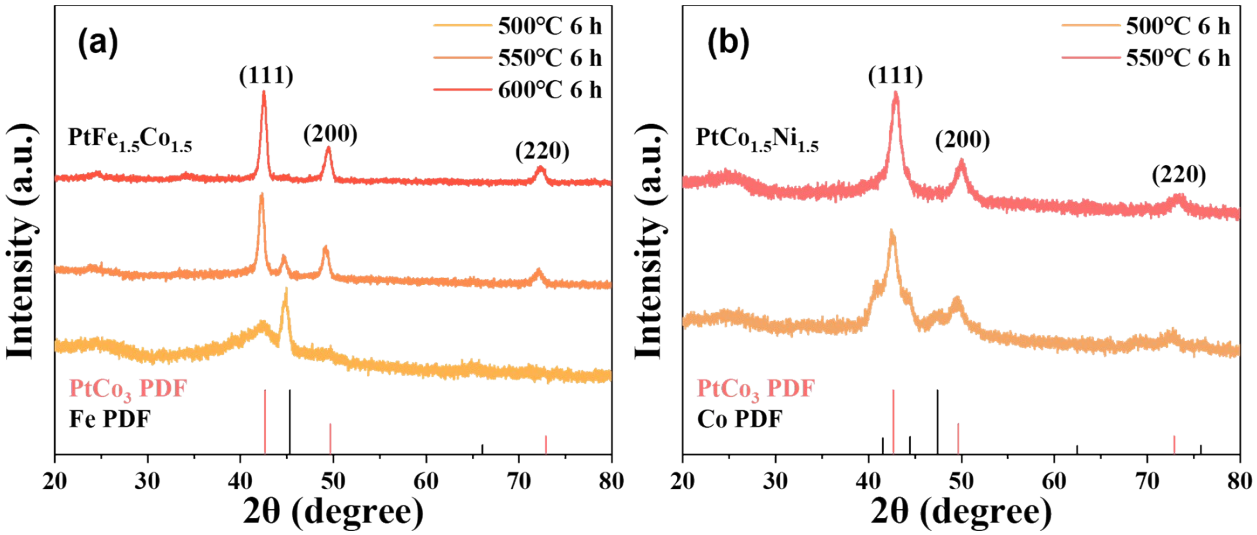

Figure S3. XRD patterns of (a) $PtFe_{1.5}Co_{1.5}$ and (b) $PtCo_{1.5}Ni_{1.5}$ annealed at different temperatures. PDF cards: $PtCo_3$ (PDF #96-152-4154), Co (PDF #04-007-7985), Fe (PDF #04-016-2968)

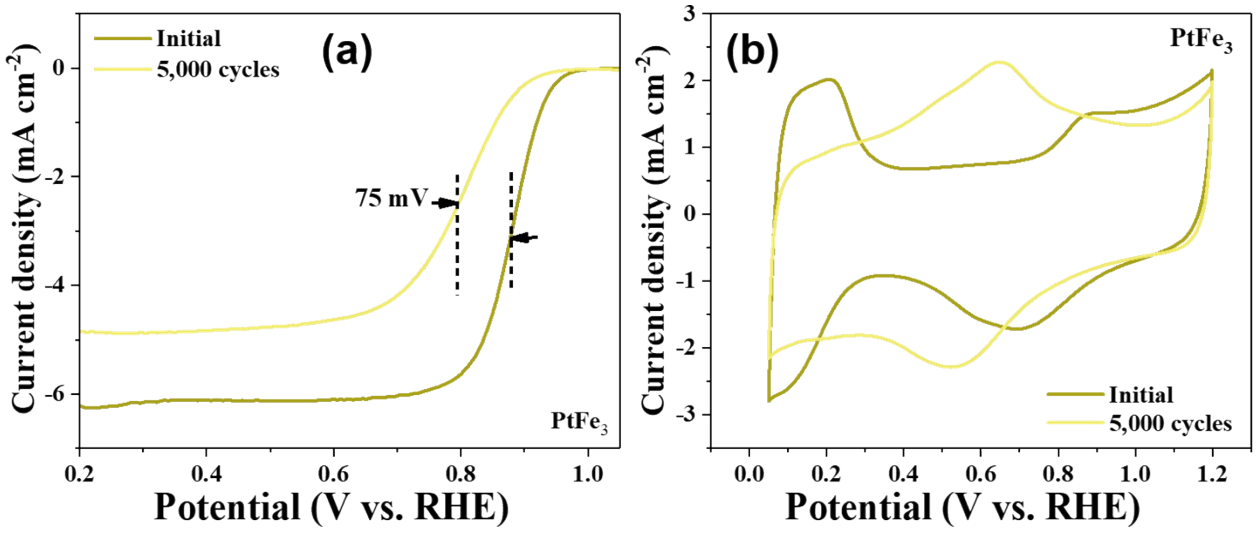

Figure S4. RDE test results of $PtFe_3$ in 0.1 mol L^{-1} $HClO_4$ at the beginning and after different cycles: (a) LSV curves; (b) CV curves.

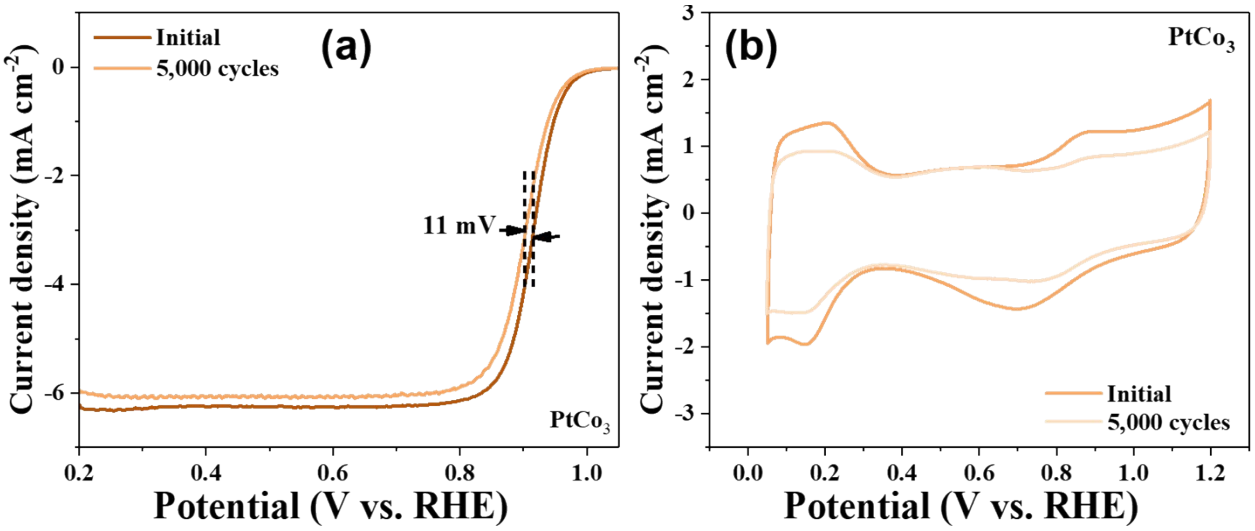

Figure S5. RDE test results of $PtCo_3$ in 0.1 mol L^{-1} $HClO_4$ at the beginning and after different cycles: (a) LSV curves; (b) CV curves.

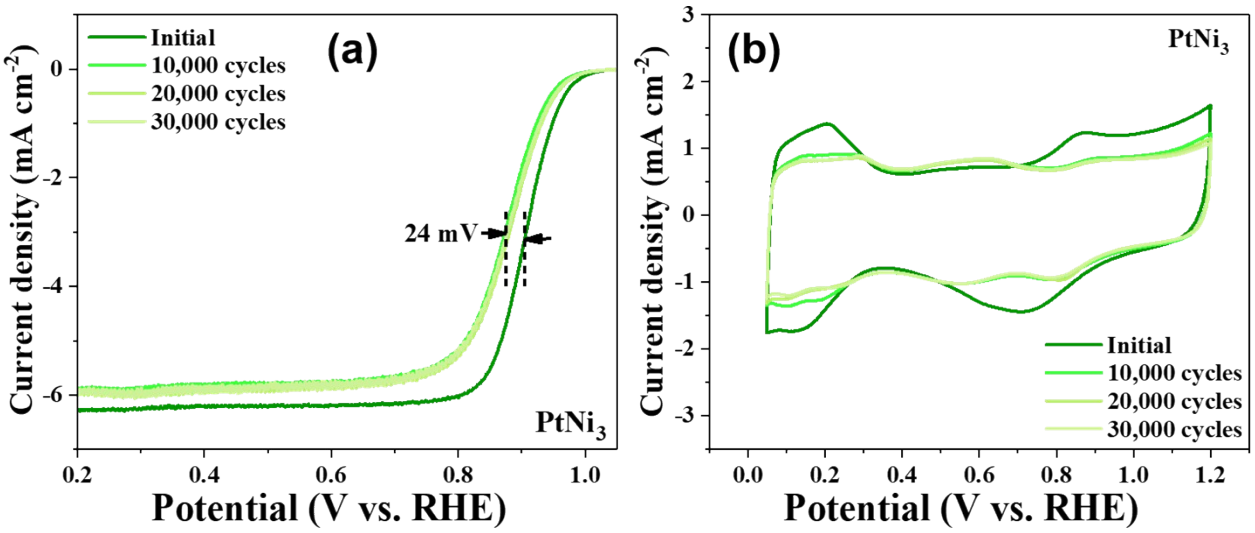

Figure S6. RDE test results of $PtNi_3$ in 0.1 mol L^{-1} $HClO_4$ at the beginning and after different cycles: (a) LSV curves; (b) CV curves.

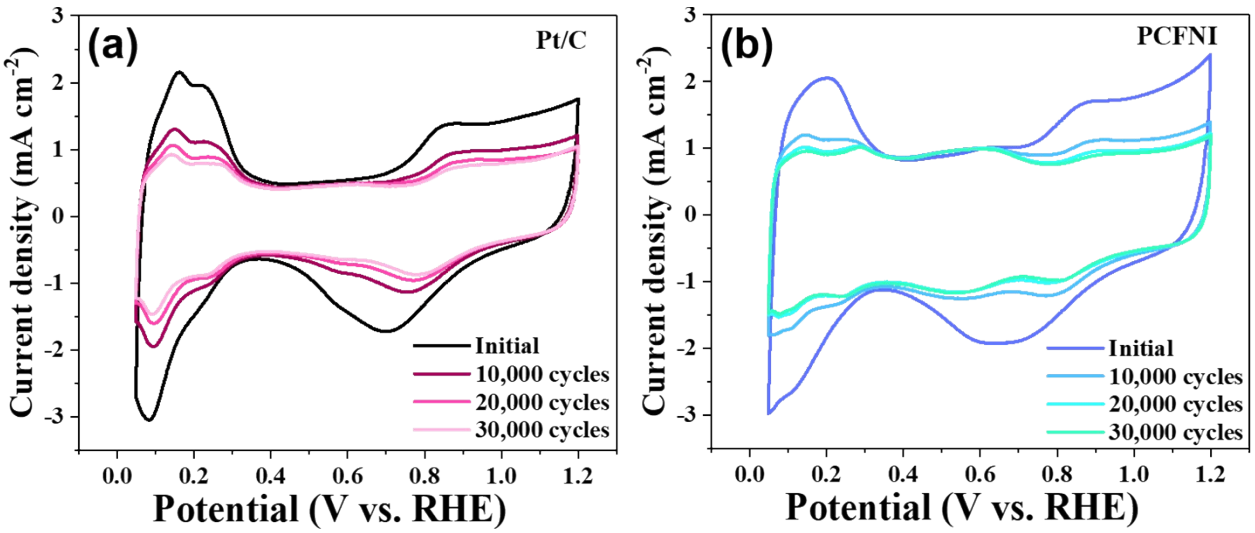

Figure S7. CV curves of (a) commercial Pt/C and (b) PCFNI tested in N_2-saturated 0.1 mol L^{-1} $HClO_4$ at the beginning and after different cycles.

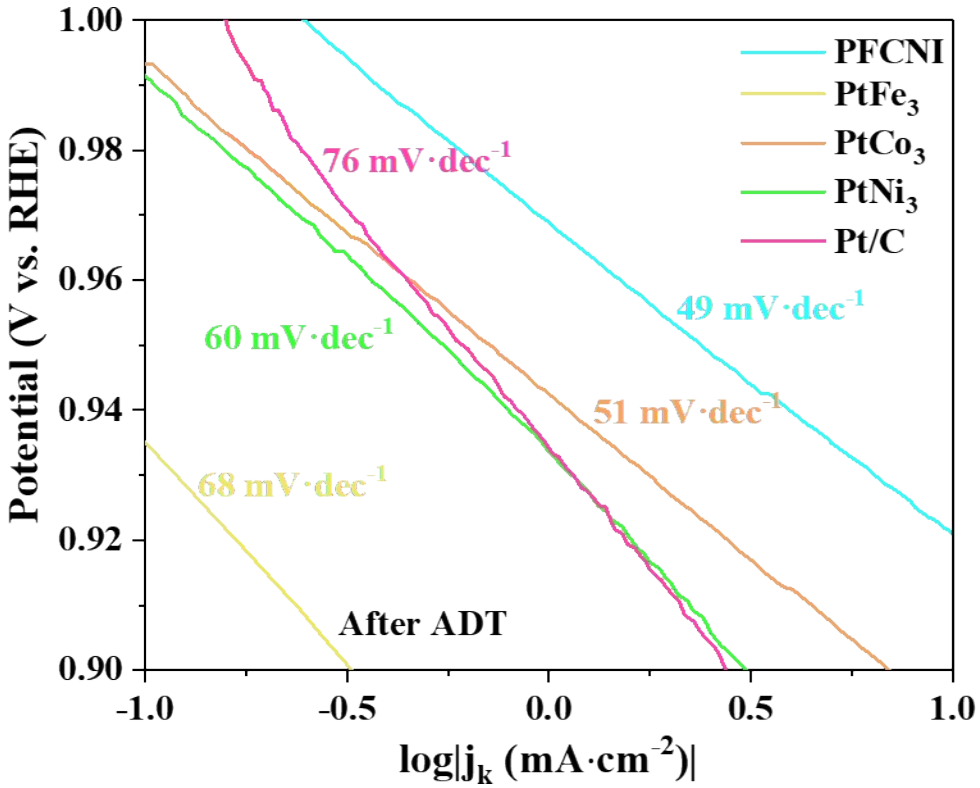

Figure S8. Tafel plots of PFCNI, $PtFe_3$, $PtCo_3$, $PtNi_3$ and commercial Pt/C tested in 0.1 mol L^{-1} $HClO_4$ after 30,000 ADT cycles.

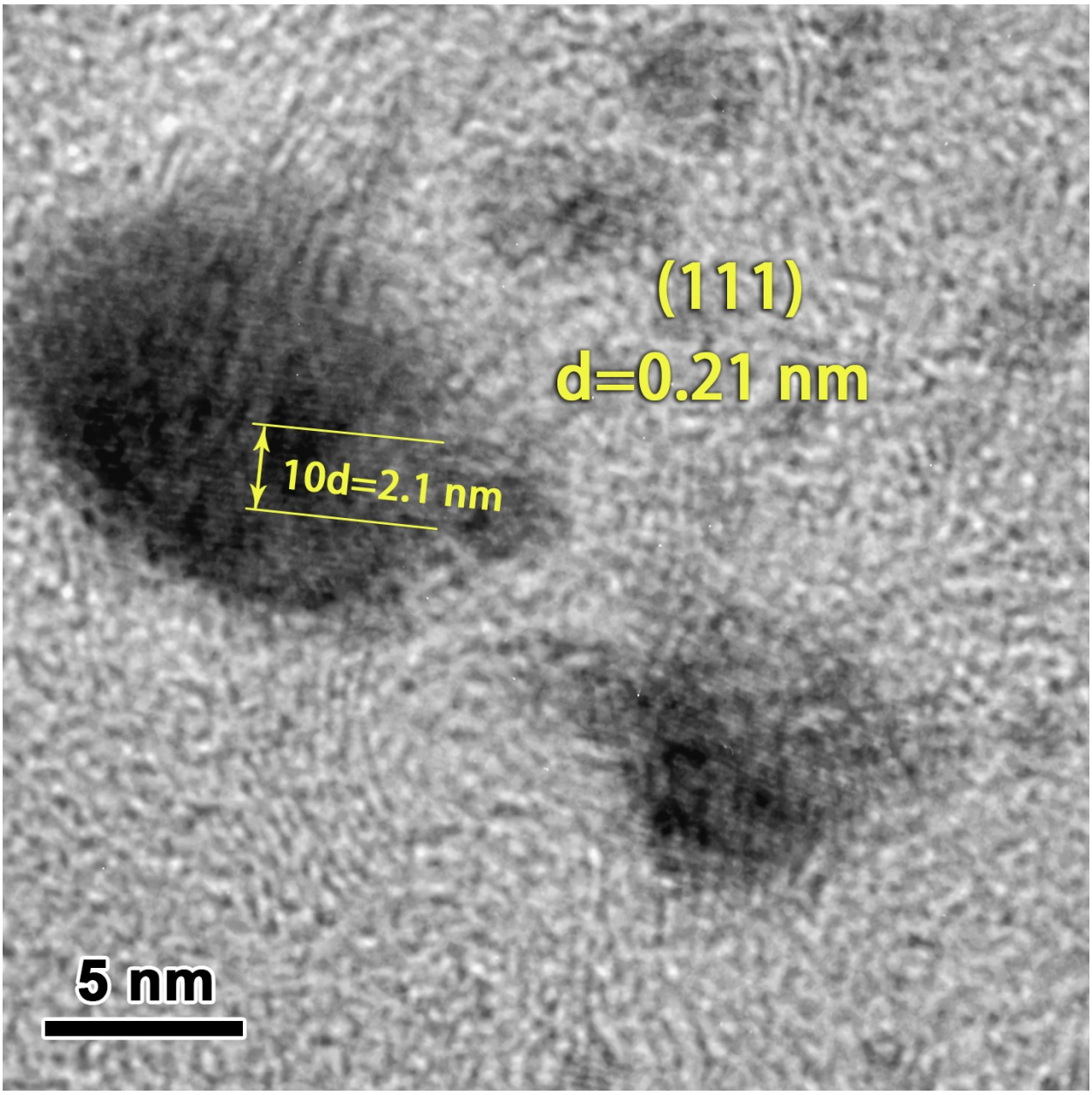

Figure S9. High-resolution TEM image of as-prepared $PtNi_3$

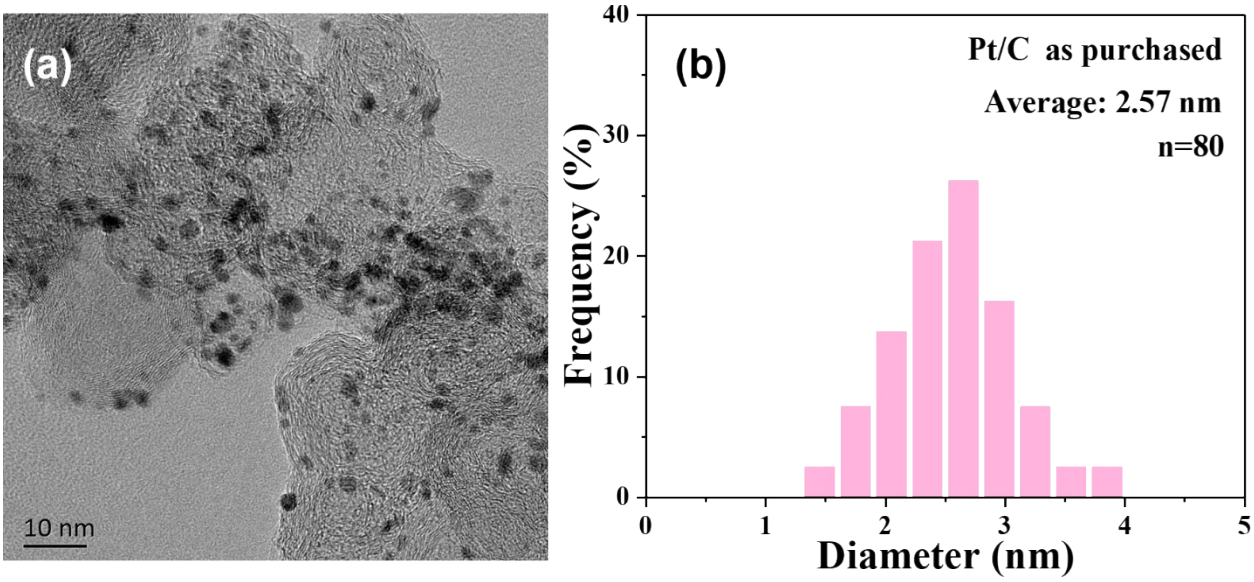

Figure S10. TEM image and particle size distribution of commercial Pt/C (as purchased)

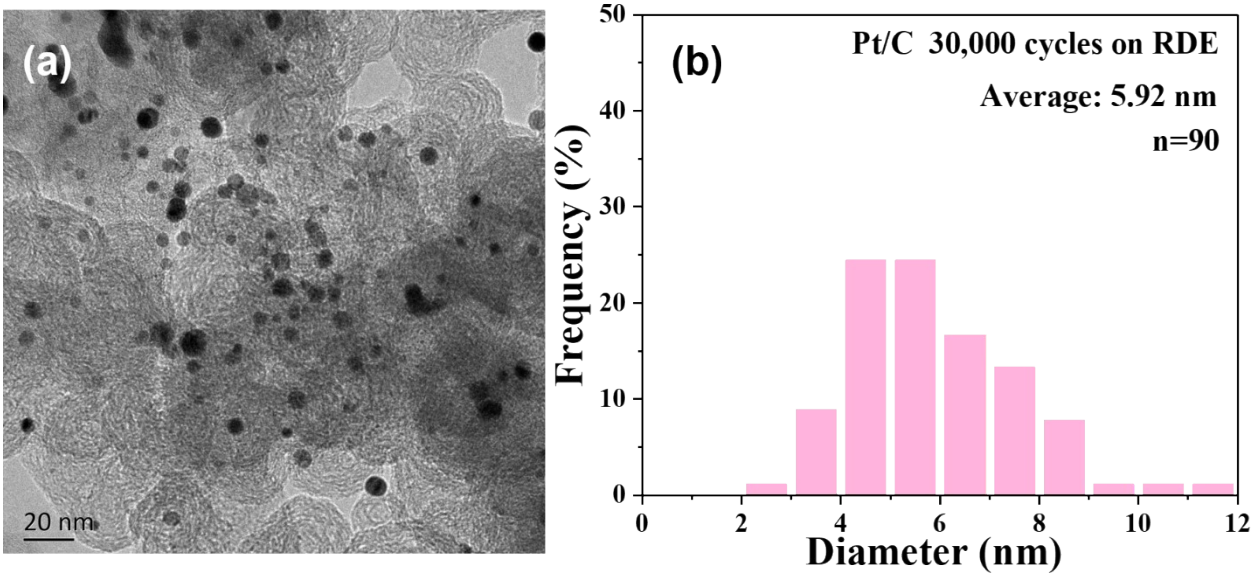

Figure S11. TEM image and particle size distribution of commercial Pt/C after 30000 cycles on RDE

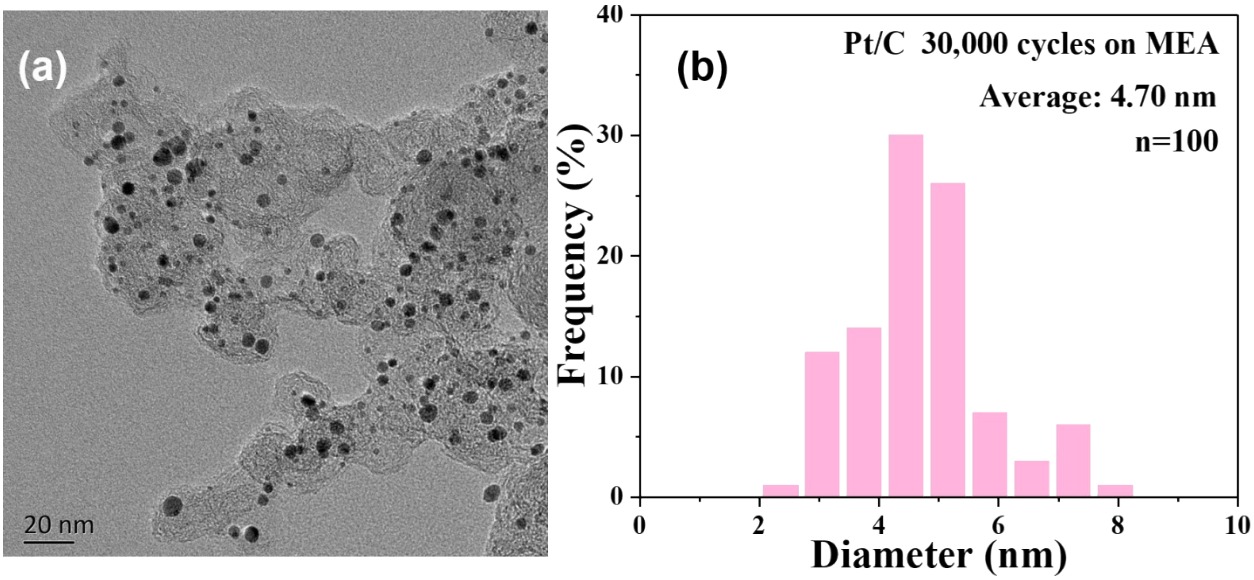

Figure S12. TEM image and particle size distribution of commercial Pt/C after 30000 cycles on MEA

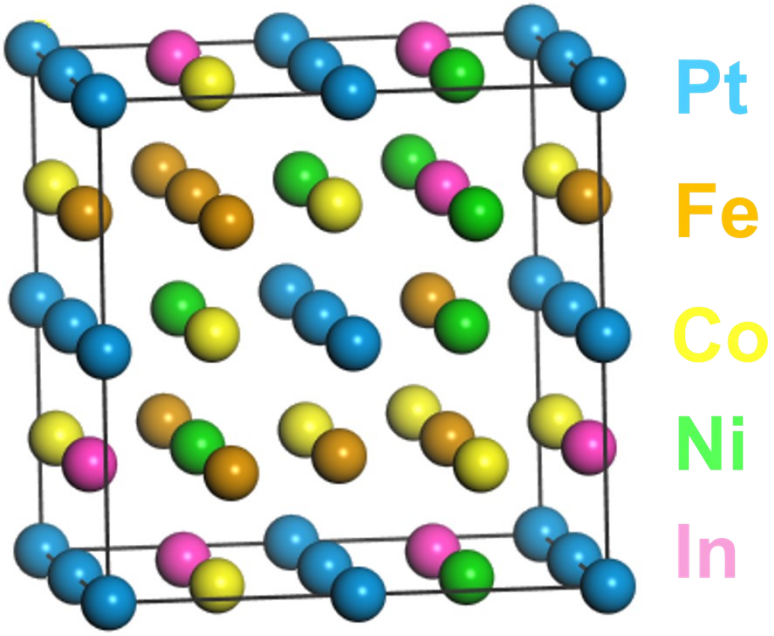

Figure S13. The 2×2×2 supercell model of PFCNI

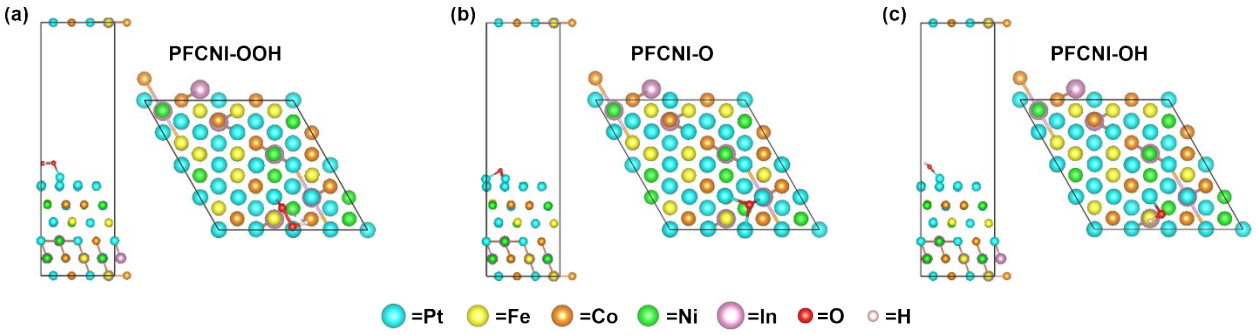

Figure S14. DFT models for surface adsorption calculation of PFCNI from the view of X and Z axis: (a) OOH*; (b) O*; (c) OH*

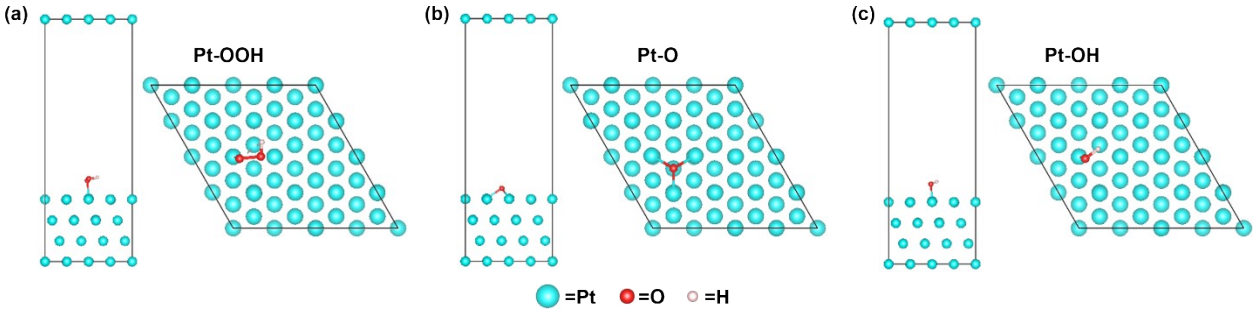

Figure S15. DFT models for surface adsorption calculation of Pt (111) from the view of X and Z axis: (a) OOH*; (b) O*; (c) OH*

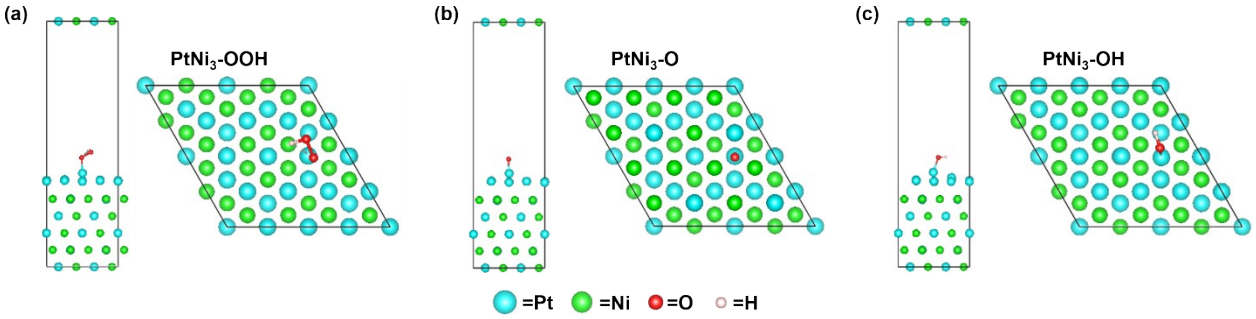

Figure S16. DFT models for surface adsorption calculation of $PtNi_3$ from the view of X and Z axis: (a) OOH*; (b) O*; (c) OH*

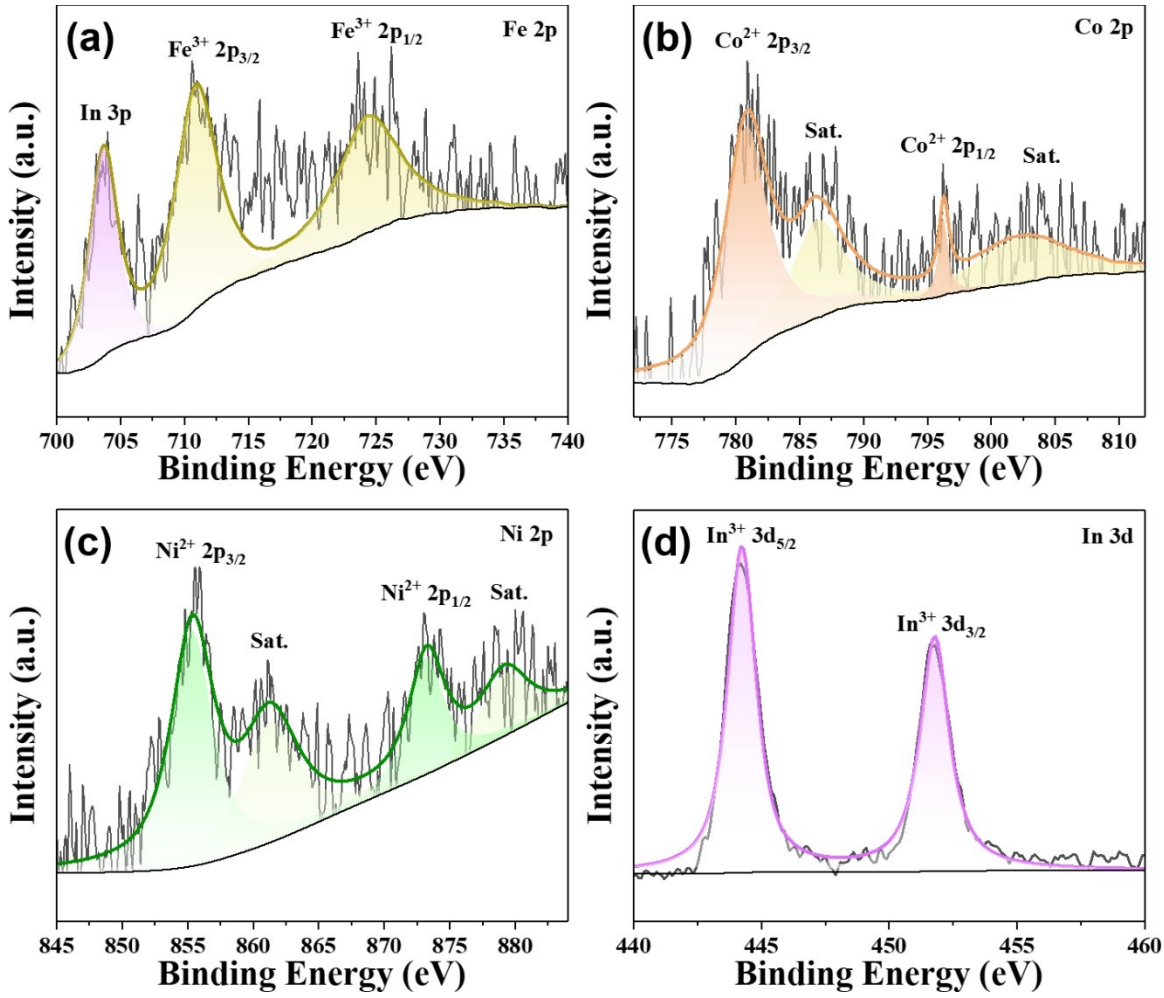

Figure S17. XPS spectra of as-prepared PFCNI measured at: (a) Fe 2p; (b) Co 2p; (c) Ni 2p; (d) In 3d

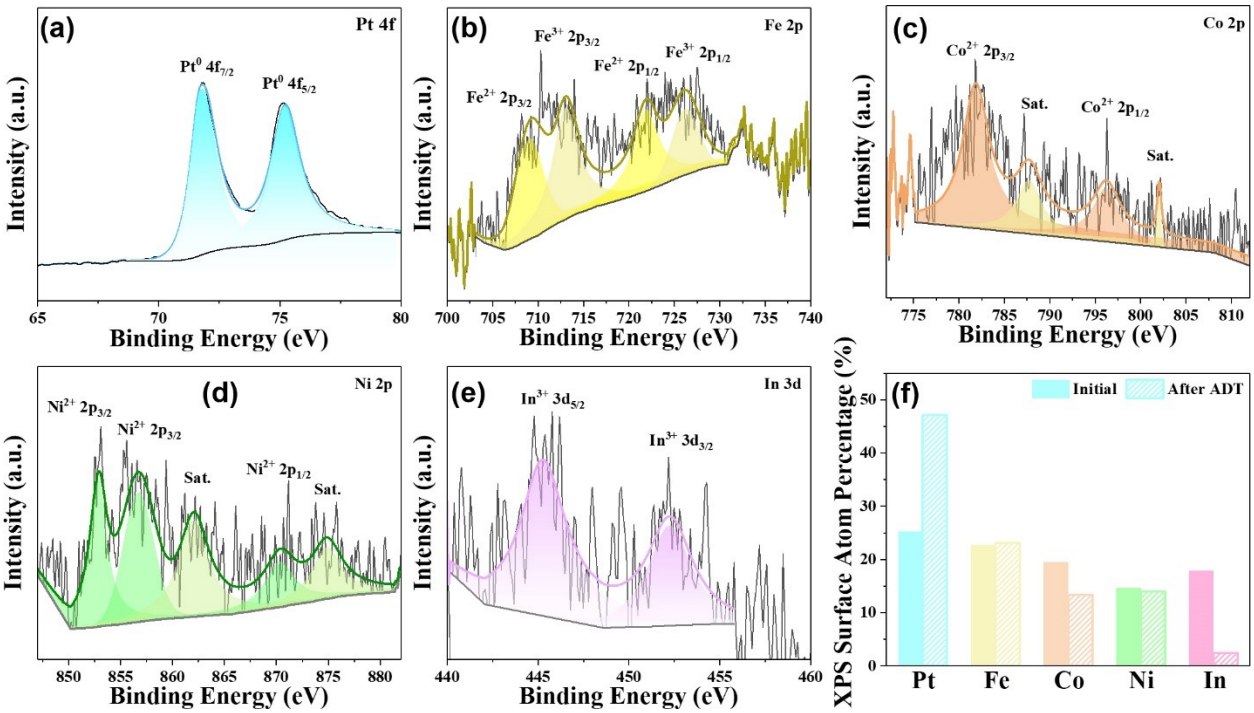

Figure S18. XPS spectra of after-cycling PFCNI measured at: (a) Pt 4f; (b) Fe 2p; (c) Co 2p; (d) Ni 2p; (e) In 3d; and (f) the comparison of XPS surface atom percentage (%) before and after cycling.

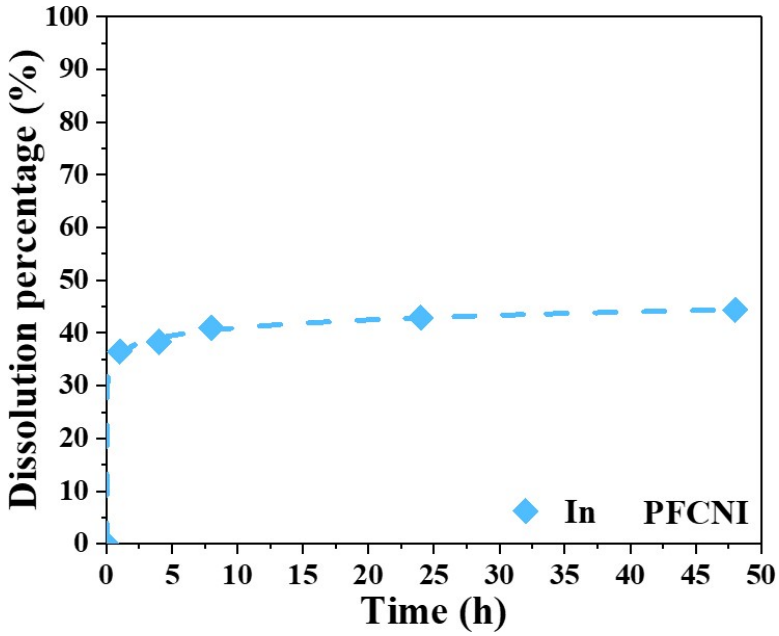

Figure S19. The corresponding In dissolution percentage measured by ICP-AES, with the as-prepared PFCNI soaked in 1 mol L^{-1} HNO_3 and sampled at 1 h, 4 h, 8 h, 24 h, 48 h

Table S1. Comparison of PtM_3 type ORR catalysts' electrochemical stability on RDE in 0.1 mol L^{-1} $HClO_4$ solution.

Catalyst (Ref.)	Initial mass activity ($A\ mg_{Pt}^{-1}$)	ADT cycles	Mass activity preservation
$PtNi_3$[1]	About 0.5~0.9	10,000	About 50%~70%
$PtNi_3$[2]	About 0.7~0.85	10,000	About 60~70%
$PtCo_3$[2]	About 0.65~0.75	10,000	About 65~80%
$PtFe_3$[2]	About 0.35~0.7	10,000	About 60~85%
O-$PtCo_3$@HNCS[3]	0.54	30,000	90.1%
Pt(Fe, Co, Ni)$_3$/C-700[4]	0.32	10,000	83%
HIFs Pt@$PtCu_3$[5]	0.36	15,000	83%
O-$PtCo_3$/C-600[6]	0.545	10,000	96.5%
O-$PtCo_3$/C-700[6]	0.447	10,000	97.5%
D-$PtCo_3$/C[6]	0.413	10,000	81.4%
PtRhNiFeCu/C[7]	1.23	10,000	75.8%
PtPdFeCoNi[8]	1.23	30,000	82.1%
PtCoNiGaZn@Pt/C[9]	0.65	20,000	73.0%

$Pt(FeCoNiCuZn)_3/C$[10]	0.70	30,000	97.1%
$PtNi_3$(This work)	0.232	30,000	41.4%
PFCNI (This work)	1.04	30,000	85.7%

REFERENCES

1. Gan, L.; Rudi, S.; Cui, C.; Heggen, M.; Strasser, P., Size-Controlled Synthesis of Sub-10 nm PtNi3 Alloy Nanoparticles and their Unusual Volcano-Shaped Size Effect on ORR Electrocatalysis. *Small* **2016,** *12* (23), 3189-96.
2. Wang, Z.; Yao, X.; Kang, Y.; Miao, L.; Xia, D.; Gan, L., Structurally ordered low‐Pt intermetallic electrocatalysts toward durably high oxygen reduction reaction activity. *Advanced Functional Materials* **2019,** *29* (35), 1902987.
3. Hu, Y.; Guo, X.; Shen, T.; Zhu, Y.; Wang, D., Hollow Porous Carbon-Confined Atomically Ordered PtCo3 Intermetallics for an Efficient Oxygen Reduction Reaction. *ACS Catalysis* **2022,** *12* (9), 5380-5387.
4. Wang, S.; Luo, Q.; Zhu, Y.; Tang, S.; Du, Y., Facile Synthesis of Quaternary Structurally Ordered L1(2)-Pt(Fe, Co, Ni)(3) Nanoparticles with Low Content of Platinum as Efficient Oxygen Reduction Reaction Electrocatalysts. *ACS Omega* **2019,** *4* (18), 17894-17902.
5. Zhang, X.; Liu, X.; Wu, D.; Hu, L.; Zhang, H.; Sun, Z.; Qian, S.; Xia, Z.; Luo, Q.; Cao, L.; Yang, J.; Yao, T., Self-Assembly Intermetallic PtCu(3) Core with High-Index Faceted Pt Shell for High-Efficiency Oxygen Reduction. *Nano Lett* **2024,** *24* (10), 3213-3220.
6. Wang, S.; Xu, W.; Zhu, Y.; Luo, Q.; Zhang, C.; Tang, S.; Du, Y., Synthesis of Structurally Stable and Highly Active PtCo(3) Ordered Nanoparticles through an Easily Operated Strategy for Enhanced Oxygen Reduction Reaction. *ACS Appl Mater Interfaces* **2021,** *13* (1), 827-835.
7. Hu, Z.; Chen, K.; Zhu, Y.; Liu, B.; Shen, J., Synergistic Effects of PtRhNiFeCu High Entropy Alloy Nanocatalyst for Hydrogen Evolution and Oxygen Reduction Reactions. *Small* **2024,** *20* (26), e2309819.
8. Yu, Y.; Xia, F.; Wang, C.; Wu, J.; Fu, X.; Ma, D.; Lin, B.; Wang, J.; Yue, Q.; Kang, Y., High-entropy alloy nanoparticles as a promising electrocatalyst to enhance activity and durability for oxygen reduction. *Nano Research* **2022,** *15* (9), 7868-7876.
9. Pan, Y.; Chen, Y.; Li, Y.; Liu, M.; Yao, L.; Zhao, H.; Zhao, X.; Yue, Z.; Gui, S.; Chen, Y.; Cheng, Q.; Yang, H., Entropy‐Increase Assisted Anti‐Sintering for Synthesis of

High‐Loaded Pt Intermetallic Compounds as Electrocatalysts in PEMFCs. *Advanced Functional Materials* **2025,** *35* (44).
10. Zhang, Q.; Shen, T.; Song, M.; Wang, S.; Zhang, J.; Huang, X.; Lu, S.; Wang, D., High-entropy L12-Pt(FeCoNiCuZn)3 intermetallics for ultrastable oxygen reduction reaction. *Journal of Energy Chemistry* **2023,** *86*, 158-166.